Veterans Administration

Journal of Rehabilitation Research
and Development, Vol. 20, No. 2
BPR 10-40 pages 15—29

Wheelchair Caster Shimmy and Turning Resistance[a]

JAMES J. KAUZLARICH, Ph. D.[b]
Professor
Department of Mechanical and
Aerospace Engineering

TED BRUNING[c]
Graduate Research Assistant
in Mechanical Engineering

JOHN G. THACKER, Ph. D.
Associate Professor
Department of Mechanical and
Aerospace Engineering

University of Virginia
Rehabilitation Engineering Center
Charlottesville, Virginia 22903

Abstract—The equations for wheelchair caster wheel shimmy are presented along with experimental data. The report includes the theory and performance of single wheel casters for a variety of tires, and a new design for wheelchair casters using a grooved dual-tread tire or co-rotating caster wheels.* The dual-tread tire was found to significantly inhibit caster shimmy.

The turning resistance due to a grooved caster wheel tire with a ½-inch groove was found to be 10 percent greater than for an ungrooved caster wheel tire. The analysis includes the methodology and the results of experiments developed to measure the sliding friction turning moment of the wheelchair caster wheel.

A number of commercial wheelchair caster wheels were tested and the results for shimmy are presented.

INTRODUCTION

The rapid side-to-side swiveling motion of a caster wheel shown in Figure 1 is called shimmy. This vibration is not a resonance phenomenon but is a self-excited motion which occurs above a characteristic critical speed of the caster wheel system, depending on the dynamics of the situation.

More than 300 books and articles have been written about shimmy since 1920, of which only a small number are concerned with wheelchair casters. Kauzlarich et al. (1), Bruning et al. (2), Brearley (3,4), Kauzlarich (5), and Thacker (6) have published wheelchair caster wheel shimmy information. Brearley made the assumption that the caster was attached to a rigid frame, which is not the case for wheelchairs. In the paper by Kauzlarich (5) the equation for the critical shimmy speed is given in which a hydraulic damper with a fixed torsional damping constant was assumed for the analysis. However, wheelchairs use frictional damping at the caster spindle, and the design equations for frictional damping are related to but differ from those for hydraulic damping. The new equations for predicting the shimmy of a frictionally damped caster wheel are presented in this paper.

ANALYSIS OF WHEELCHAIR CASTER SHIMMY

Purpose

It is the purpose of this section to present the shimmy equations for predicting the critical speed at which wheelchair caster shimmy begins for frictionally damped casters, and to include the effect of a grooved tire, or co-rotating pair of tires. It is intended that these equations will give the designer sufficient information to avoid the problem of caster wheel shimmy.

[a]This work was supported by the National Institute for Handicapped Research Grant No. G00-8300-72.

[b]Dr. Kauzlarich may be addressed at Thornton Hall, University of Virginia, Charlottesville, Virginia 22901. Telephone (804) 924-6218 or 977-6730. His other published papers are in areas of friction, wear, lubrication, heat transfer, design, and fluid mechanics. He is the inventor of a welding machine, hydraulic bearings, and a medical catheter.

[c]Ted Bruning is an engineer with IBM Corporation, Tucson, Arizona.

*Patent pending

Model

Bruning (7) found that when the caster went into shimmy the frame also vibrated, and that for small-angle shimmy there was no measurable indication that the caster wheel slipped on the floor in its lateral vibration. For the low speeds of wheelchairs with their relatively rigid caster-wheel tires, a simple two-degree-of-freedom model is adequate. The model assumes that the tire tread may or may not be separated by a groove or that co-rotating wheels may be a part of the design. The plan view of the model is shown in Fig. 2. If the groove width $B=0$, the model will give results for a single-tread wheel. As shown in the model, when the caster wheel is deflected sideways a restoring normal force F_N is developed between the wheel and floor. In addition, for co-rotating wheels, a restoring moment is produced by the frictional forces F_T acting on both treads due to the rotation of the caster wheel about the spindle axis as it is deflected. If the wheels were not co-rotating the latter restoring moment would not exist. In the case of a single wheel the restoring moment due to rotation when deflected is negligible for wheelchair casters.

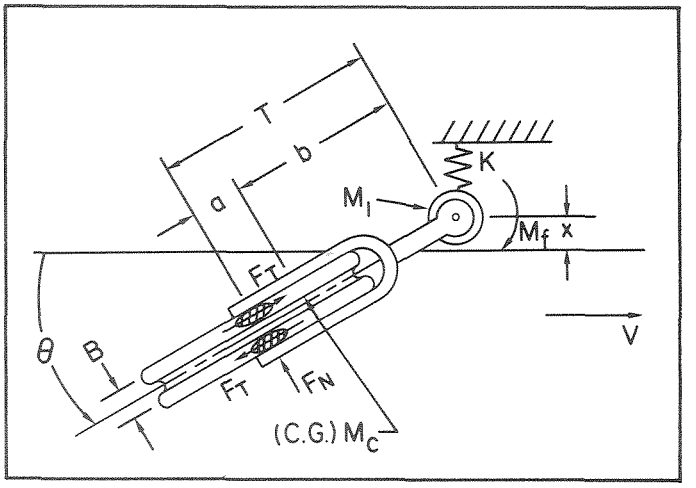

FIGURE 2
Caster wheel model.

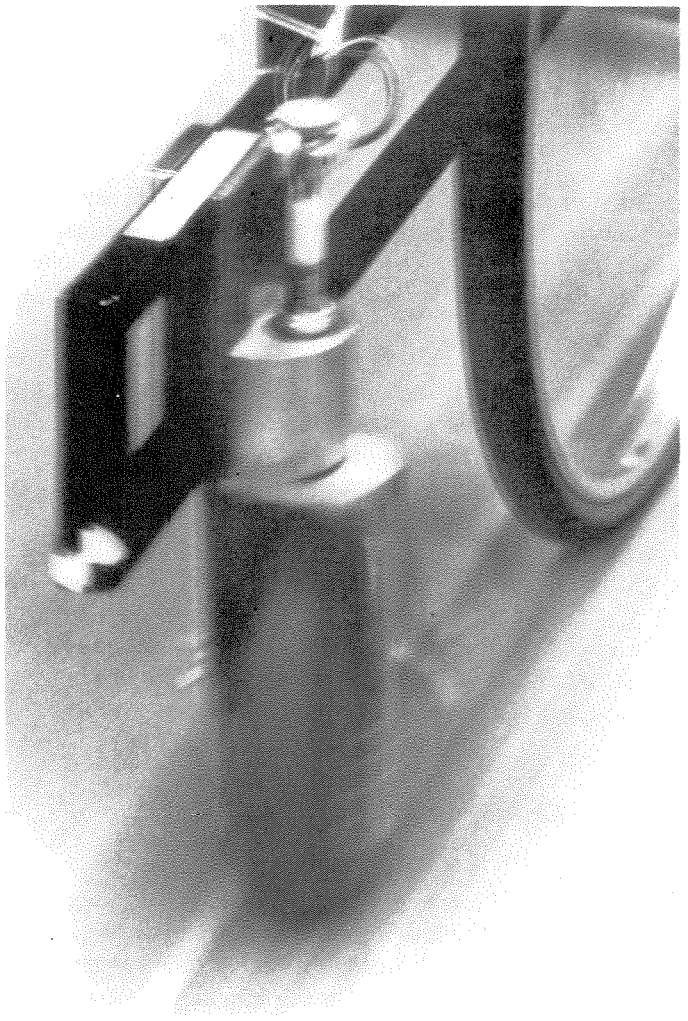

FIGURE 1
Shimmying caster.

Frictional damping is assumed to take place between the spindle and caster bearing block. The wheelchair frame exerts a lateral restoring spring force on the bearing block which can be measured directly in terms of stiffness K. The apparent mass of the bearing block M_1 is determined by measuring the lateral natural frequency of the frame, bearing block, and spindle bearings system (without the caster wheel and fork) and applying the equations of simple spring-mass vibration. The mass moment of inertia of one wheel about a diameter, I_W, and its mass, M_W, are needed for the calculations. The usual small angle assumptions are used in the analysis.

Design Equations

In designing a wheelchair caster, considerations of strength and size as well as shimmy must be investigated. For example, the equation for the force per unit load, P/L, needed to push a caster wheel over a threshold, where d/h is wheel diameter to threshold height, (see Appendix A) is given by

$$\frac{P}{L}=\frac{2\sqrt{\frac{d}{h}-1}}{\frac{d}{h}-2}\cong 2\sqrt{\frac{h}{d}} \qquad [1]$$

A graph using Equation [1] (see Appendix A) shows that, for a small threshold height on the order of ½ inch P/L increases rapidly for wheel diameters below 6 inches. Although strength and dynamic performance are necessarily a part of the design, only the design for shimmy will be considered further in this paper.

The differential equation (see Appendix B) for the model shown in Figure 1 is third order, and has a solution of the form:

$$\theta = C_1 e^{\lambda t} + e^{\mu t}(C_2 \sin \omega t + C_3 \cos \omega t) \qquad [2]$$

Equation [2] gives the angular position θ of the caster wheel as a function of time t. The angular frequency of the shimmy vibration is ω. $C_{1,2,3}$ are constants determined by the initial conditions for the problem. For a differential equation with positive coefficients, the first term of Equation [2] is transient and dies out quickly. The exponent μt controls the motion of the caster and can be positive or negative. When $\mu = 0$ this is at the onset of shimmy.

The coefficients $C_{1,2,3}$ of Equation [2] are determined by assuming an initial deflection of the caster wheel θ_0 due to a bump on the floor. The resulting equation which is valid for $\mu = 0$, at the transition from stable to self-excited motion, is

$$\frac{\theta}{\theta_0} = \frac{\omega^2 \frac{T^2}{v^2} e^{-\frac{v}{T}t}}{1 + \omega^2 \frac{T^2}{v^2}} + \frac{1}{\sqrt{1 + \omega^2 \frac{T^2}{v^2}}} \cos(\omega t - \phi) \quad [3]$$

The wheelchair speed is v, the caster trail is T, and ϕ is the phase lag of the vibration.

The first term in Equation [3] approaches zero in less than one cycle for a typical wheelchair caster, so that [3] can be simplified to

$$\frac{\theta}{\theta_0} \cong \frac{v}{\omega t} \text{Cos}(\omega t - \phi). \quad [4]$$

By applying the Hurwitz-Routh stability criterion to the differential equation (see Appendix D) for the model, where damping at the spindle is assumed to have a hydraulic damping coefficient C_D, an equation governing the onset of shimmy is developed as

$$V_c^2 - \frac{C_D T V_c}{I_w} - \frac{K_s B^2 T}{2 I_w} = 0 \quad [5]$$

In Equation [5] V_c is the critical velocity at the shimmy threshold, B is the width of the tire groove, K_s is the tire slip coefficient, and I_w is the wheel moment of inertia about its diameter. Equation [5] can be reduced to the case for a frictional damper with a constant resisting torque or moment of M_f by using a relation between frictional and hydraulic damping (See Appendix C) of

$$C_D = \frac{4M_f}{\pi \theta_a \omega} \quad [6]$$

The amplitude of shimmy θ_a is obtained from Eq. [4].

Substituting Equation [6] into Equation [5] using results from Equation [29 B] (see Appendix B) gives the governing equation for the onset of caster shimmy:

$$V_c^2 = \frac{4M_f T^2}{\pi \theta_0 I_w} + \frac{K_s B^2 T}{2 I_w} \quad [7]$$

K_s was found to be on the order of 1250 newtons (see Appendix C) for wheelchair tires. The tests show that $M_f/\theta_0 = 1.3$ N-m/rad. for the ball-bearing test fork used (see Appendix C).

Experimental Results

Bruning (7) investigated shimmy performance of several commercial wheelchair casters, including the effect of a ¼-inch groove in an Everest & Jennings 7½-inch solid gray rubber-tire wheel. The data points are plotted (as points) in Figure 3 where the solid and dashed lines are the theoretical curves using Equation [7]. The theory and the experiment are seen to be in good agreement.

Figure 4 gives the theory (solid and dashed lines) and the test data points for an Invacare 7¾-inch semi-solid polyurethane tire caster wheel with and without a ½-inch groove in the tire. The plot shows good agreement between the theory and experiment.

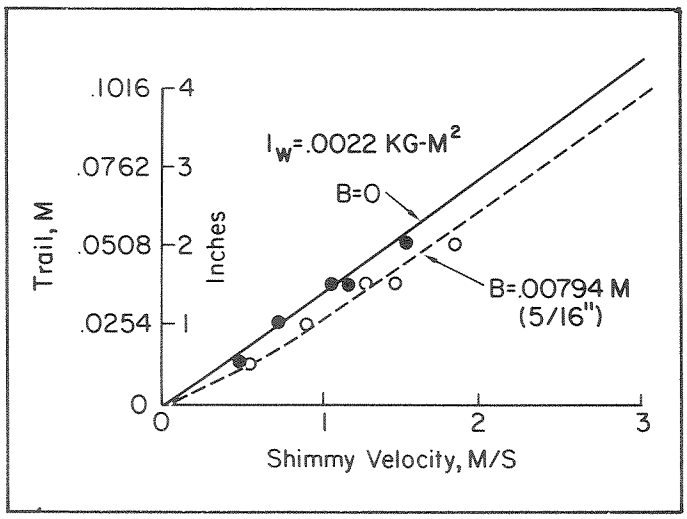

FIGURE 3
E&J 8-inch solid gray rubber tire caster wheel; data points vs. theoretical curves.

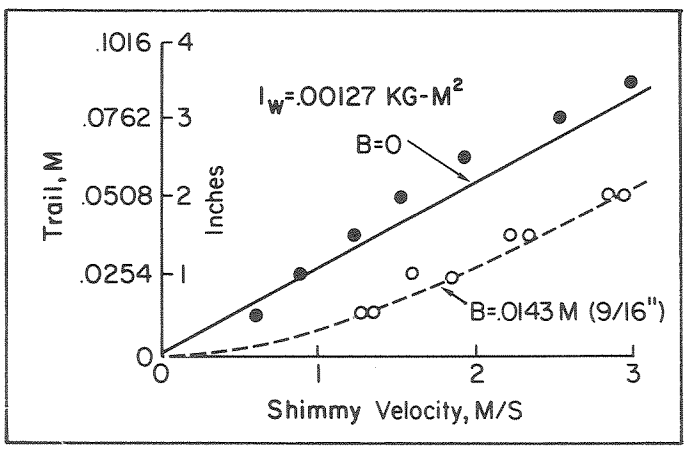

FIGURE 4
Invacare 8-inch semi-solid polyurethane tire caster wheel; data points vs. theoretical curves.

A sample calculation using Equation [7] at a data point in Figure 4, for the curve B = 9/16 inches with a trail of 2 inches, is shown below.

$$V_c^2 = \frac{4(1.3)(.0508)^2}{\pi .00127} + \frac{1250(.0143)^2\ .0508}{2(.00127)} \qquad [8]$$

$$V_c = 2.91\ m/s\ (16.86\ mph)$$

Discussion

An evaluation of the existing theories of caster wheel shimmy was presented by Smiley (8) in 1957, including the third order system used in the analysis of this report, but excluding the tire groove effect. His analysis shows that this theory, which is one of the simplest models, applies well to caster wheels with relatively rigid tires, which exhibit low critical shimmy speeds.

TURNING RESISTANCE DUE TO A GROOVED WHEELCHAIR CASTER WHEEL

Background

At low speeds, maneuverability is hindered by the caster's frictional resistance to turning about the caster axis: large values of torque must be applied to the handrim to overcome this turning resistance. (In many instances, the wheels are not rotating when a turn is attempted.) Stout (9) measured the turning friction by setting the caster wheels straight ahead and measuring the force applied at the front of the frame necessary to laterally move the frame ½ inch. Tests similar to Stout's were conducted by Kauzlarich (10) with respect to electric powered wheelchairs.

To eliminate the problem of wheelchair caster shimmy, Kauzlarich (5) determined that a grooved caster-wheel tire significantly inhibits caster shimmy. He showed that the speed necessary to initiate shimmy with a grooved tire is much higher than the normal operating speed of the wheelchair. Thus, grooved tires will effectively increase wheelchair stability and decrease power consumption. The question that must be answered is, what penalties must be paid for these benefits? The major penalty turns out to be the increased turning resistance due to the grooved tire. An analysis of this problem is the subject of this section of the paper.

Materials and Methods

Two caster wheels were used in the study. Both of the 7¾-inch-diameter tires were made of polyurethane, but with different cross-section geometry (Fig. 5). Two modes of tire turning were investigated. The first test measured the sliding friction turning moment necessary to turn a non-rotating wheel on tile and carpet surfaces. The second experiment measured the force which had to be provided by the wheelchair occupant to turn an experimental wheelchair frame as the caster wheel trail was varied and as the caster load varied.

1. Measurements of sliding friction turning moment—To determine the sliding friction turning moment, the caster wheel was mounted in a drill-press using an experimental fork. The caster trail in these tests was set to zero. A platform scale was placed on the drill-press table and the different materials (tile and short pile carpet) were placed between the scale and the wheel (Fig. 6). The thrust mechanism on the drill-press spindle was used to apply constant normal loads to the wheel, and the platform scale indicated the magnitude of the caster load. A force to turn the wheel was applied to the experimental fork, level with the wheel axis, and perpendicular to the spindle axis of the drill press. A spring scale was used to measure the magnitude of this force.

The results of the test are given in Figure 7, which gives the sliding friction turning moment versus normal caster load for three types of wheels on vinyl tile and short pile carpet. The sliding friction turning moments for carpet are approximately double the turning moments on tile partially because the carpet tended to build up in front of the caster wheel. The grooved caster required 30 percent more torque than the standard Everest and Jennings gray rubber wheel and 10 percent more torque than the ungrooved wheel made of the same material.

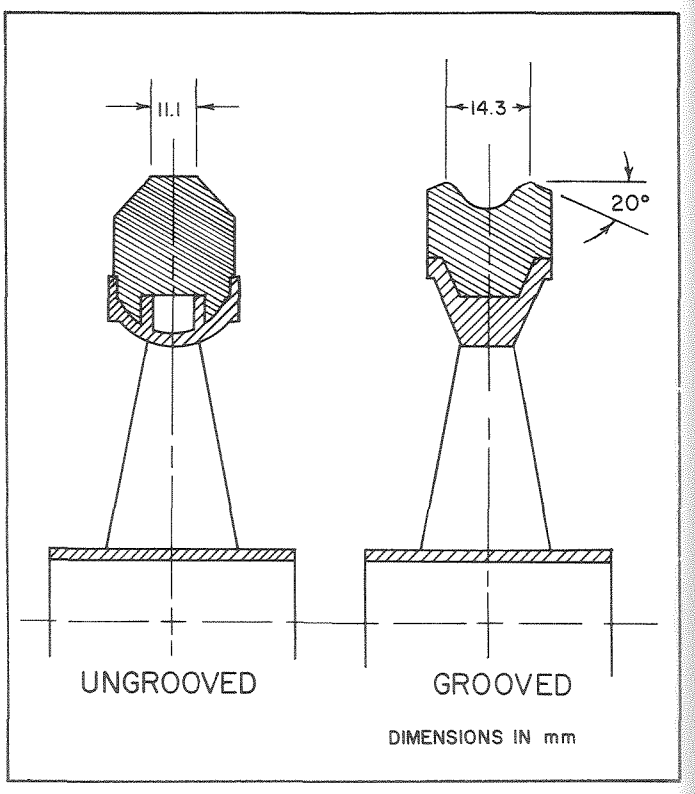

FIGURE 5
Caster wheel tire cross sections.

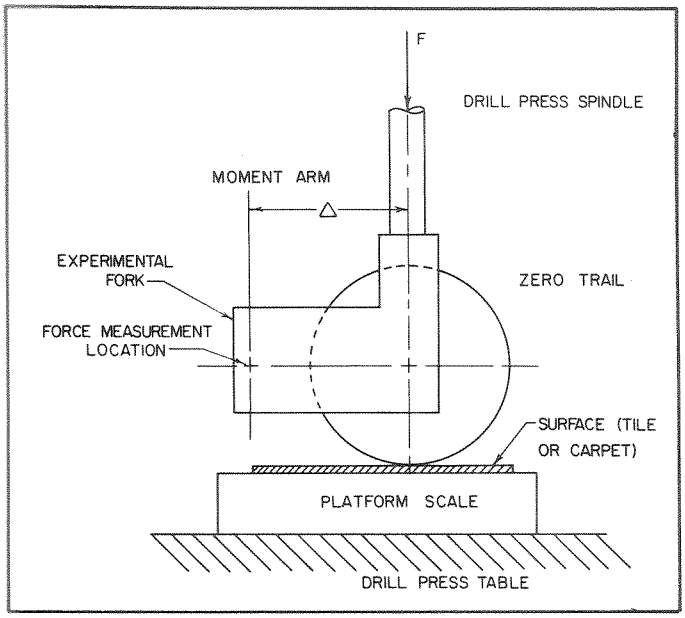

FIGURE 6
Drill-press measurement of caster wheel turning resistance.

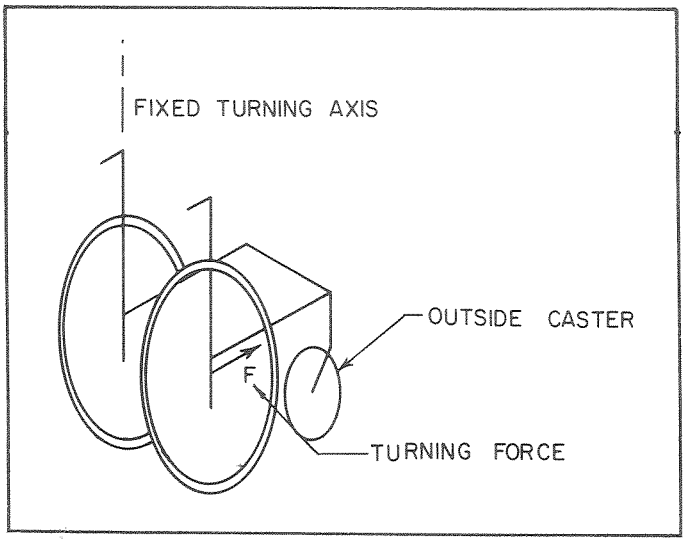

FIGURE 8
Wheelchair turning resistance measurement.

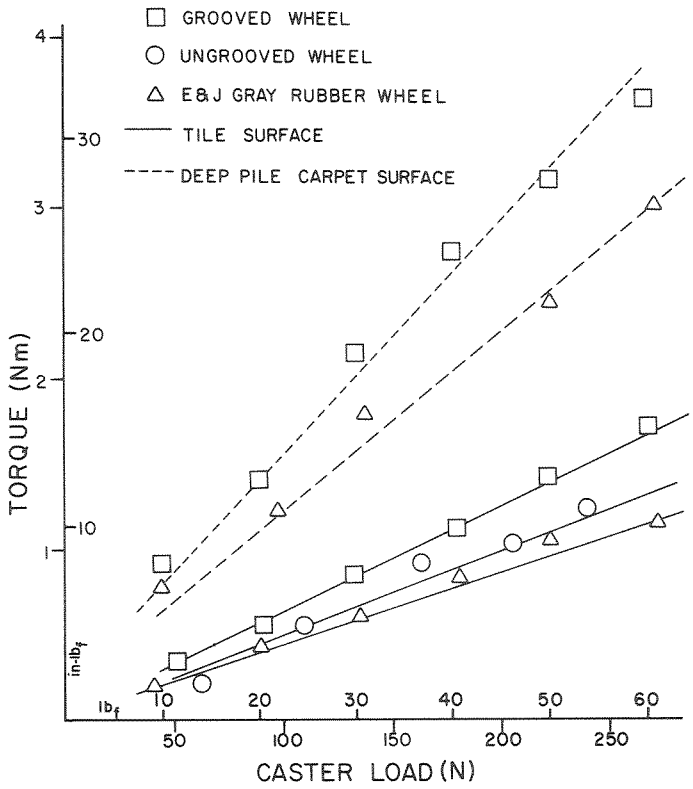

FIGURE 7
Drill-press caster wheel turning resistance for tile (A) and carpet (B).

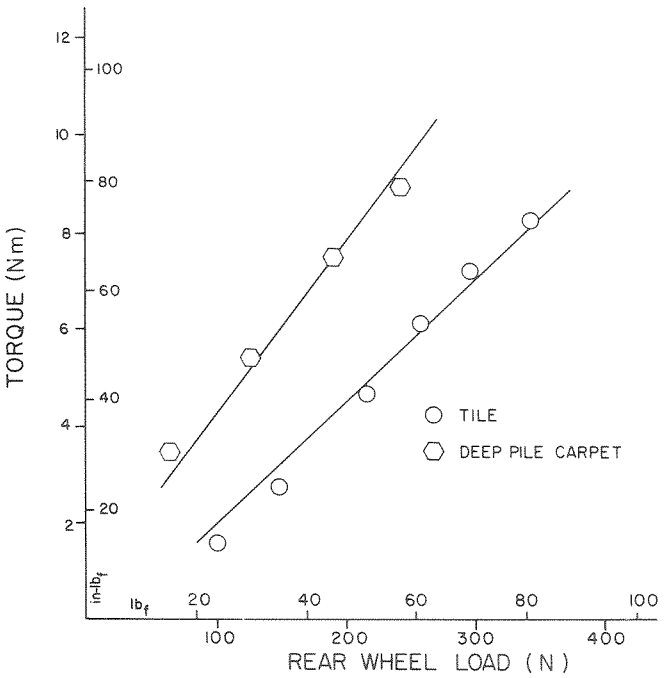

FIGURE 9
Wheelchair rear wheel sliding friction turning moment.

2. Force required to turn a wheelchair—To gain insight into the actual performance of the grooved tire, a test was performed in which the wheelchair was constrained to pivot (without rolling) about the right rear wheel. The tires were Silver Star Gum Walls. A horizontal force perpendicular to the axle was applied to the left rear axle outboard of the wheel (Fig. 8). The front two casters were set straight ahead, and the force necessary to initiate turning as well as to continue turning was measured.

The sliding turning moment for the pivoting rear wheel is given in Figure 9. The force applied to the left rear axle to initiate turning (10 degrees maximum) is given in Figure 10.

A corresponding turning moment about the caster axis was calculated from the measured force shown in Figure 9. It was assumed that the friction turning moment in the bearings of the caster assembly is much less than the friction turning moment between the wheel and surface. A free-body analysis of the experimental wheelchair frame

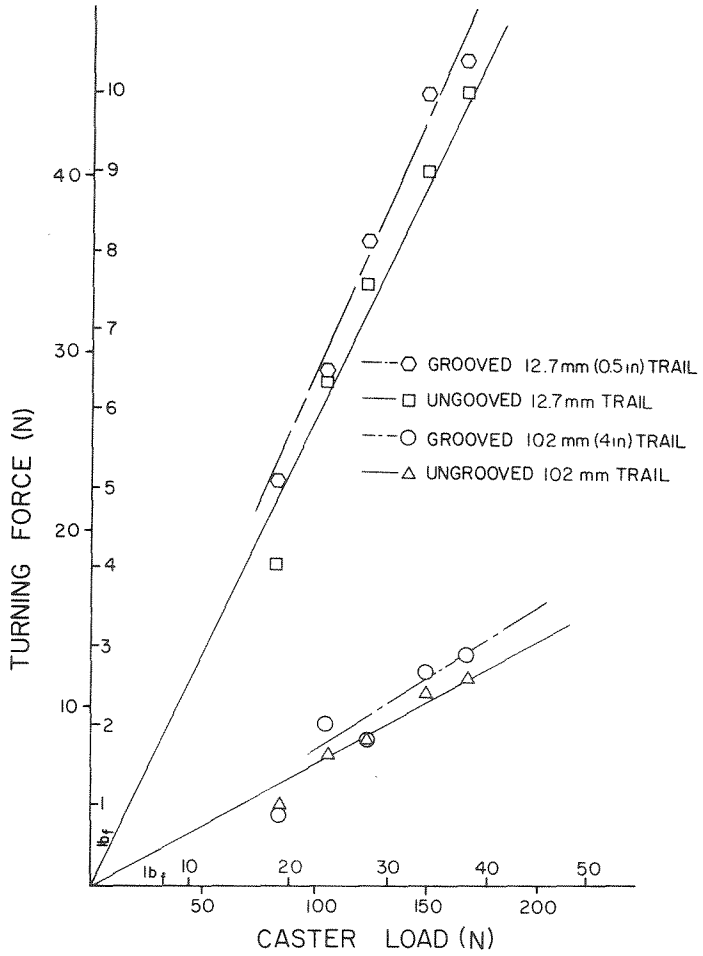

FIGURE 10
Force to initiate wheelchair turning versus load and trail.

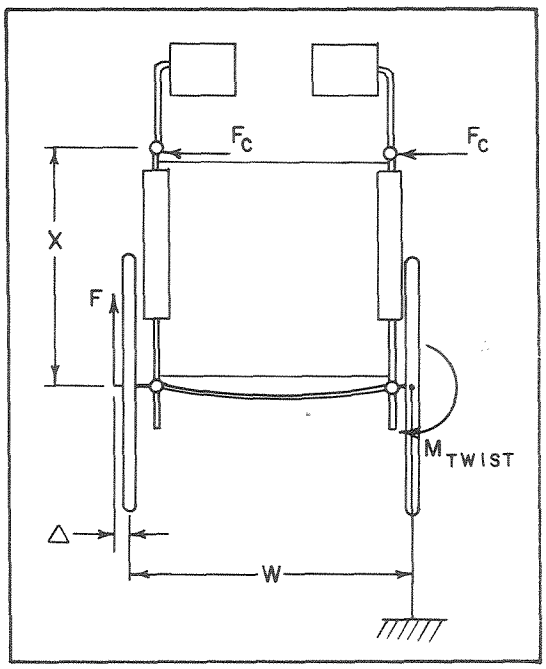

FIGURE 11
Wheelchair turning resistance test model.

(Fig. 11) gives the magnitude of the horizontal force F_c applied at each caster axis. Summing moments about the stationary rear wheel:

$$F_c = \frac{F\,(W + \Delta) - M_{Twist}}{2X} \qquad [9]$$

where, the experimentally measured force (Figure 10), is F, the width between the two rear wheels is W, the distance from the center of turning wheel to the point of application of the measured force is Δ, the distance to the caster axis from the twisting rear wheel is X, and the twisting moment is M_{Twist}.

Although the trail of the caster assembly was varied, the position of the caster wheel relative to the center of mass of the chair remained constant. Hence, for different trail lengths, the distance X to the front caster axis varied. Once F_c was determined using Equation [9], the turning moment was calculated by multiplying the value of F_c by the trail length. It is found that this turning moment is about 50 percent of the value obtained from the non-rolling sliding turning test using the drill press. The grooved wheels require about 10 percent extra effort over the ungrooved wheels. Although the magnitudes of the torques are different, the drill press test gave the same

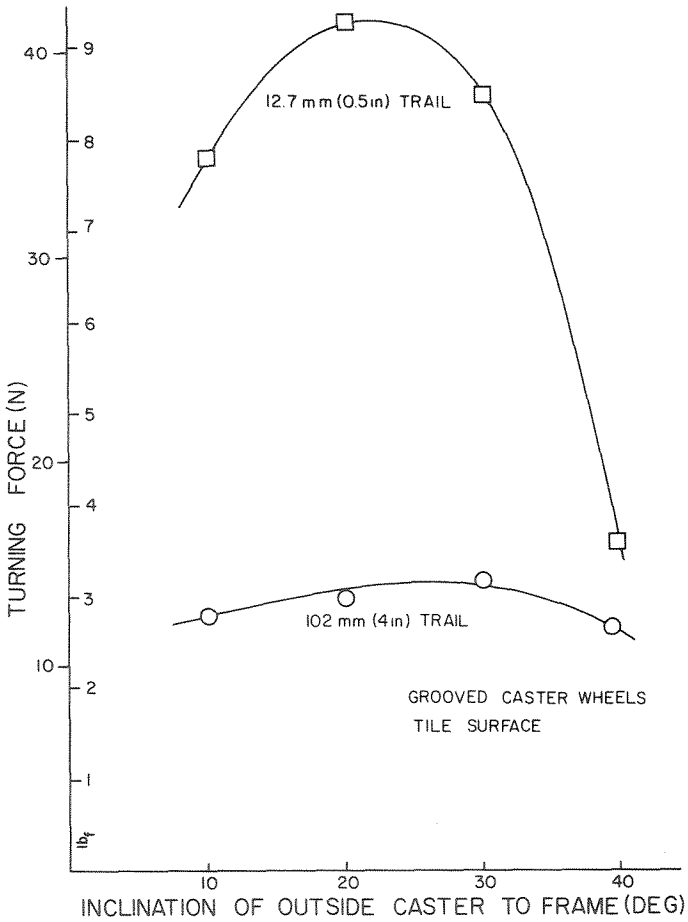

FIGURE 12
Force to Continue Turning Wheelchair.

relative difference (10 percent) in performance.

Figure 12 illustrates the force necessary to continue turning the chair. It was observed that the initial effort required to turn the wheelchair is not necessarily the maximum effort required. The length of trail roughly correlates to the effort needed to turn the wheelchair; that is, doubling the trail length will decrease the effort by a factor of two.

THE EFFECT OF INERTIAL PARAMETERS OF COMMERCIAL WHEELCHAIR CASTERS ON CASTER SHIMMY

Shimmy is one of the more important problems of wheelchairs, because it can cause a significant increase in rolling resistance which can lead to loss of control and stuctural failure of the wheelchair. A study of wheelchair caster shimmy at the Rehabilitation Engineering Center (7) has identified inertial characteristics of commercial caster wheels that contribute significantly to the tendency to shimmy.

Wheelchair Caster Wheel Shimmy

Shimmy is a self-excited vibration caused by a force that is a function of the state of the system itself, rather than being caused by an external periodic force. In the case of wheelchair caster shimmy the force is a function of the angular position of the caster, the transverse acceleration of the wheelchair frame, and the forward speed of the wheelchair. When the caster wheel is pointed exactly in the direction of motion of the wheelchair, there is no driving force for shimmy and the caster will not shimmy. However, if there is any disturbance that causes a deviation of direction or a transverse acceleration of the wheelchair frame, shimmy may begin.

When the vibration is initiated, its amplitude will either diminish and cease or it will increase and persist; the outcome depends strongly on the speed of the wheelchair, the torsional damping, and the inertial characteristics of the caster. Sustained shimmy occurs at higher speeds. At lower speeds the shimmy will damp out; the lower the speed the more rapidly the shimmy subsides.

Tests and Results

Tests were run with a specially built wheelchair tethered on a treadmill. The test wheelchair had an adjustable caster fork as shown in Figure 13 which allowed changes in the trail of the caster wheel without changing the wheelchair.

The spindle of the fork rotates in a pair of sealed ball bearings and no frictional damping other than that of the ball bearings was used. Tests (7) show that commercial forks and the test fork gave practically the same results when the spindle bearings were the same and additional friction was omitted.

Stability, or the ability to roll without shimmy, was

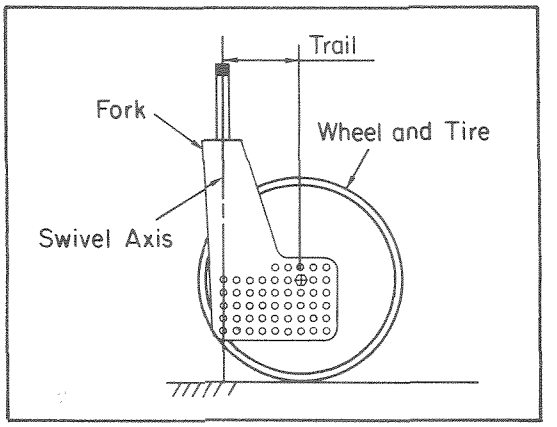

FIGURE 13
Test fork.

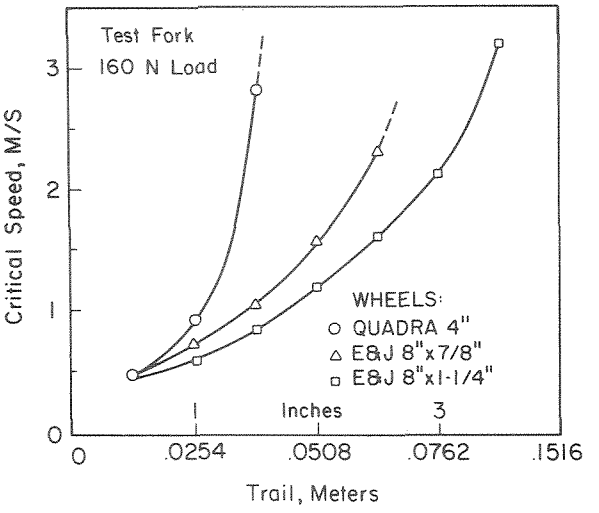

FIGURE 14
Wheelchair shimmy speed versus trail.

measured by determining the critical velocity for the caster wheel being tested; this is the speed below which the vibration damps out and above which the vibration is sustained. The inertial parameters included in the study were the masses and the moments of inertia of the fork and the wheel, and the location of the centers of gravity of the fork and the wheel with respect to the swiveling axis.

The stability of casters depends strongly on two of the inertial characteristics of the casters. The first is the trail of the caster, and the second is the moment of inertia of the wheel about a vertical axis through its center of gravity.

In one set of tests, a variety of commercial wheelchair caster wheels were used with the test fork shown in Figure 13. The axle of the wheel was placed in the test fork at different locations to vary the trail without changing any of the other parameters. Figure 14 is a plot of the critical speed as a function of trail for three different wheels, using the test fork. As the trail increases, the critical velocity increases exponentially. In these tests the spindle bearing friction has increased with trail.

TABLE 1
Caster wheel parameters

		Diameter meters (in.)	Mass kg	Moment of Inertia kg-m²	Critical speed @2" trail m/s
A	Quadra	.1016 (4)	.280	.18	Stable*
B	Kryptonics (MOD.)	.1270 (5)	.338	.33	Stable*
C	E & J (Mod.)	.1778 (7)	.444	1.07	2.39
D	PRC Pneumatic	.2032 (8)	.562	1.25	1.77
E	Stainless	.2032 (8)	.815	1.60	1.46
F	E & J 8 × 7/8	.2032 (8)	.699	2.00	1.58
G	E & J 8 × 1¼	.2032 (8)	1.380	3.42	1.20

*up to 3.8 m/s (13.7 km/hr)

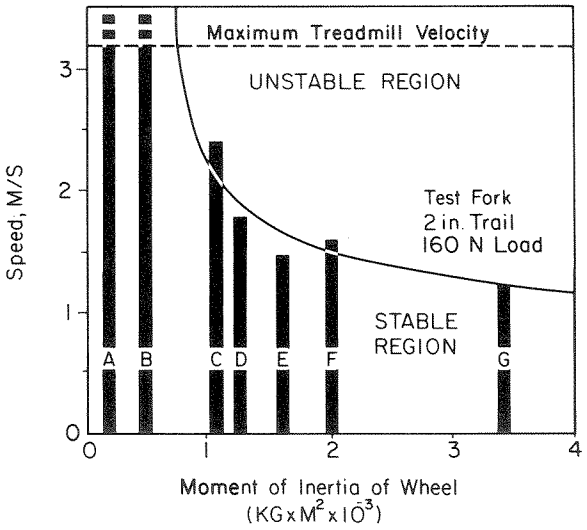

FIGURE 15
Wheelchair shimmy speed versus wheel moment of inertia. Key letters refer to table 1.

The forks supplied by the manufacturers have trails of between 2.00 and 2.25 inches. At moderate walking speed, which is about one meter per second (2.24 mph), the two Everest & Jennings wheels in the test fork are operating near to the critical speed. At higher speeds (a brisk walk or a coast down a hill) those wheels are very likely to shimmy unless damping is increased. The Quadra wheel, with its low moment of inertia (see Table 1) is sold in a fork with trail of 2.50 inches, and as a result it never operates close to the critical speed and never shimmies, a feature that makes it popular with wheelchair-basketball players.

In another test, a variety of wheels were placed in the test fork with a trail of 2.0 inches and a load of 160 newtons (35.9 lb). In Figure 15, the range of velocity for stable operation is plotted for each of the wheels listed in Table 1 against the moment of inertia of the wheel. For wheels A and B which have a low moment of inertia, there was no tendency to shimmy at the maximum treadmill speed of 3.8 meters per second. The wheels with low moment of inertia have smaller diameter and least mass as seen in Table 1.

Discussion

For the tests just described and for similar tests investigating the effect of other variables, the values for the parameters were varied across a range that includes all wheelchair casters in current use. Within that range, only the trail and moment of inertia of the wheel (of the six parameters investigated) significantly contributed to the stability of the caster. This result is in agreement with the theory of Equation [7] for fixed M_f and $B = 0$.

There are, however, numerous non-inertial factors which affect stability. The load on the caster, the shape and composition of the tire, and the fit and drag of the bearings are among the list of additional factors that affect stability. As a result, testing and design of casters should consider these factors as well as the inertial parameters.

Conclusion

In conclusion, the onset of self-excited vibration of wheelchair caster wheels can be avoided by modifying the design of the caster wheel assembly. The equations show that increasing the trail, decreasing the moment of inertia of the wheel, increasing the damping and/or adding a groove in the tire, will inhibit the onset of shimmy. All of these effects have been demonstrated experimentally and the results agreed well with the theory.

The grooved caster wheels require approximately 10 percent extra effort when the user is attempting to turn the wheelchair on a rigid surface. A simplified test using a drill press, platform scale, and spring scale can be used to give meaningful information about the relative turning resistances of different caster wheels

Two inertial parameters of commercial wheelchair casters, the trail and the moment of inertia of the wheel, strongly influence the tendency of the caster to shimmy. Careful attention to the values of these parameters enable the design of a caster that will not shimmy in everyday use. Resistance to shimmy is enhanced by maximizing the trail and minimizing the moment of inertia of the wheel. Increasing caster-spindle frictional damping also inhibits caster shimmy, but at the expense of increased caster turning effort ■

Appendix A

NECESSARY FORCE TO PUSH A WHEEL OVER A THRESHOLD

The smaller the caster wheels of a wheelchair, the greater is the force that is required to push the wheel over a threshold. This force is a nonlinear function of the threshold height and is dependent upon the speed of the wheelchair.

The equation for the force per unit load at the lowest possible speed is derived using the model shown in Figure 1 A. For this three-force system, the lines of action of the forces must be coincident at the axle. the maximum value for the force P occurs when the wheel just begins to lift from the floor and the floor load N is zero. As the wheel is pushed over the threshold the force P decreases.

For static equlibrium

$$\Sigma F_x = -P + R\cos\theta = 0 \qquad [1A]$$

$$\Sigma F_y = -L + N + R\sin\theta = 0 \qquad [2A]$$

$$\frac{P}{L} = \frac{1}{\tan\theta} = \frac{\sqrt{\left(\frac{d}{2}\right)^2 - \left(\frac{d}{2} - h\right)^2}}{\frac{d}{2} - h} \qquad [3A]$$

$$\frac{P}{L} = \frac{2\sqrt{\frac{d}{h} - 1}}{\frac{d}{h} - 2} \qquad [4A]$$

$$\frac{P}{L} \cong 2\sqrt{\frac{h}{d}} \qquad [5A]$$

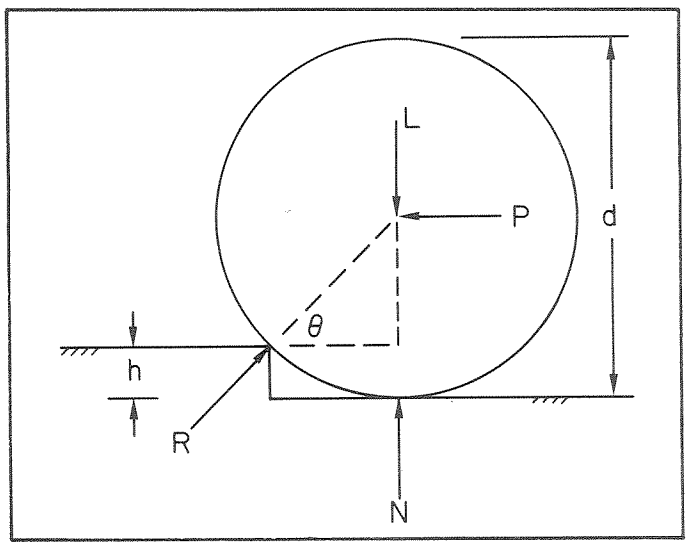

FIGURE 1A
Wheel forces at a threshold.

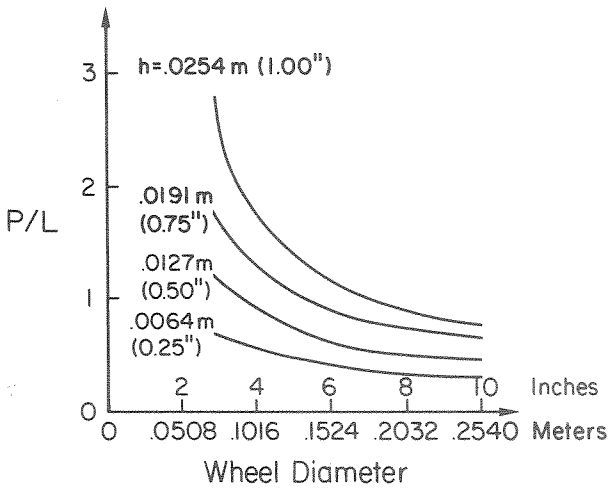

FIGURE 2A
Force per-unit-load necessary to traverse a threshold.

A feeling for the maximum force necessary to surmount a threshold is obtained from the results shown in Figure 2A. The plot of P/L shows that as the diameter of a caster wheel gets larger and approaches the typical size for wheelchairs of 8 inches, the maximum force per unit load necessary to cross a threshold approaches a minimum asymptote. However, as the diameter of a caster wheel increases its moment of inertia also increases and the caster wheel is then more prone to shimmy. Thus, as in most designs, the design of the caster wheel is a compromise of competing requirements.

Note that the analysis is for the force P at the axle of a wheel. Further analysis is necessary to couple this result to a wheelchair application where the resultant force on the wheel axle will not be horizontal.

APPENDIX B

CASTER WHEEL SHIMMY THEORY

The derivation of the equations of caster wheel shimmy follows the method presented by Moreland (11), in part.

The plan view model of a caster with two co-rotating wheels is shown in Figure 1B with all of the forces and moments (including inertia terms of importance) for describing the dynamics of the problem. The caster wheel is shown in a deflected position with a restoring force F_N acting at the wheels. This two-degrees-of-freedom model involves lateral motion in the X direction and rotational motion in the θ direction. The angular inertia force is I_G and the lateral inertia force is M_cX_G. The wheelchair frame acts as a spring with spring constant K to produce a spring force KX, while the casterfork spindle bearing-block exerts an inertia force M_1X. Damping is assumed to take place at the caster-fork spindle and the damping opposes the

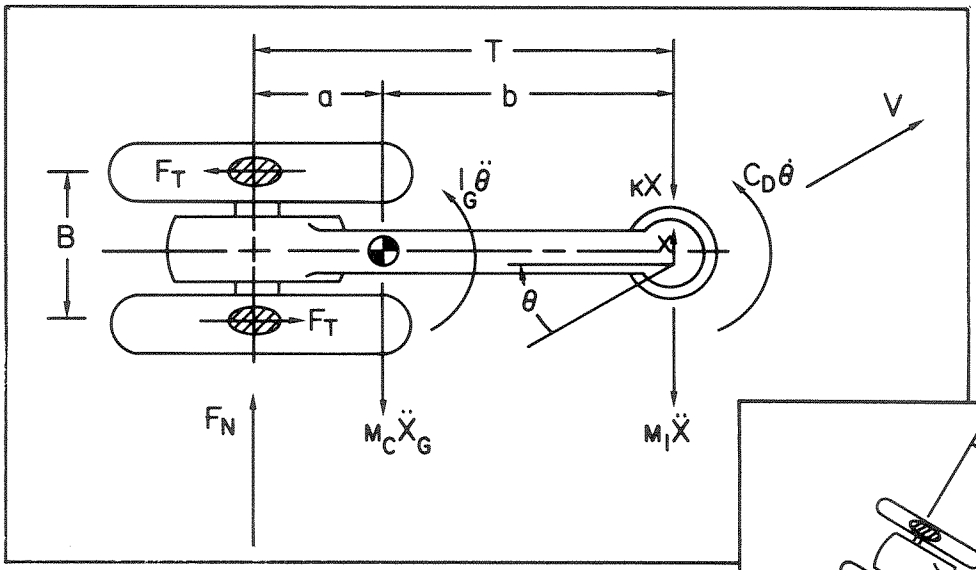

FIGURE 1B
Caster wheel force diagram.

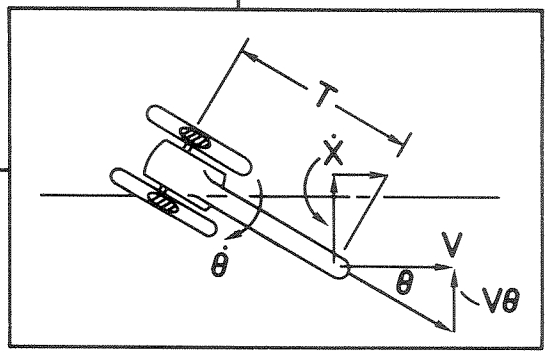

FIGURE 2B
Kinematics of swiveling caster wheel.

angular motion of the wheel and fork by $C_D\dot{\theta}$. The damping is assumed to be velocity-dependent hydraulic damping, with a constant coefficient of C_D. (A conversion to frictional damping is considered later. The assumption at this point of hydraulic damping simplifies the analysis.) The two wheels are assumed to be connected to a rigid axle which requires co-rotational rolling. The two wheels are separated by an effective ground contact width B. A force F_T acts between the co-rotating wheels and the floor, due to the angular velocity $\dot{\theta}$ of the caster wheel when it is angularly deflected, which exerts an added damping torque to the caster. One can observe this effect by twisting a pair of wheels locked to a common axle. However, if the wheels are allowed to rotate independently, twisting the axle is observed to experience no resistance. Thus, the non-co-rotating caster wheels used on several models of childrens' strollers will not exert a force F_T at each wheel, and the added damping torque does not exist. When the wheel separation B is zero, a single tread wheel is modeled and the damping moment at the wheel contact with the floor is negligible. The trail T is the distance between the wheel-tread contact with the floor and the spindle. The distances a and b identify the position of the center of gravity of the caster wheel and fork assembly as shown.

The force F_T is described by Stevens (12) in terms of a wheel slip coefficient K_s and the change in velocity of the wheel due to F_T ratioed with the velocity of the wheelchair as follows.

$$F_T = K_s \frac{\Delta V}{V} = \frac{K_s B\dot{\theta}}{2V} \qquad [1B]$$

Thus the torque or moment due to F_T acts to restore the caster wheel to its undeflected position and is

$$M_{F_T} = F_T B = \frac{K_s B^2\dot{\theta}}{2V} \qquad [2B]$$

Including Equation [2B], the system equations for the caster wheel can be written as follows.

$$F_N - (KX + M_1\ddot{X}) = M_C\ddot{X}_G = M_C(\ddot{X} + b\ddot{\theta}) \qquad [3B]$$

$$aF_N + b(KX + M_1\ddot{X}) - C_D\ddot{\theta} - \frac{K_S B^2\theta}{2V} = I_G\ddot{\theta} \qquad [4B]$$

Equations [3B] and [4B] can be combined by eliminating F_N between them giving

$$a(KX + M_1\ddot{X}) + aM_C(\ddot{X} + b\ddot{\theta}) + b(KX + M_1\ddot{X}) + (C_D + \frac{K_S B^2}{2V})\dot{\theta} = I_G\ddot{\theta} \qquad [5B]$$

The kinematics of the caster swiveling about the fork spindle and advancing at wheelchair velocity V is shown (exaggerated) in Figure 2B.

The relative velocity at the wheel trail of the caster with respect to the spindle, assuming small angles of rotation, is

$$-T\dot{\theta} = \dot{X} + V\theta \qquad [6B]$$

Differentiating Equation [6B] gives

$$\ddot{X} = -T\ddot{\theta} - V\dot{\theta} \qquad [7B]$$

Substituting Equations [6B] and [7B] into [5B], differentiating the resulting equation, and using [6B], gives

$$(I_G + M_C a^2 + M_1 T^2)\,\dddot{\theta} + (C_D + aM_C V + M_1 TV + \frac{K_S B^2}{2V})\,\ddot{\theta} + KT^2\dot{\theta} + KTV\theta = 0 \quad [8B]$$

Equation [8B] can be simplified by assuming that the mass of the caster is concentrated at the wheel and at the spindle such that

$$a = T\frac{M_f}{M_C} \text{ and } b = T\frac{M_w}{M_C} \quad [9B]$$

$$M_C = M_f + M_w \quad [10B]$$

If the moment of inertia of the fork about its own axis is negligible in comparison to the moment of inertia of the wheel, then

$$I_G = I_w + M_w a^2 + M_f b^2 = I_w + T^2\frac{M_f M_w}{M_C} \quad [11B]$$

Using Equations [9B] [10B] and [11B] to simplify Equation [8B], get

$$(I_w + (M_f + M_1)\,T^2)\,\dddot{\theta} + (C_D + (M_f + M_1)\,TV + \frac{K_S B^2}{2V})\,\ddot{\theta} + KT^2\,\dot{\theta} + KTV\theta = 0 \quad [12B]$$

Dividing through by the coefficient on $\dddot{\theta}$, and recognizing that the resulting coefficient on $\dot{\theta}$ gives the square of the natural frequency of this third-order linear differential equation,

$$\dddot{\theta} + \frac{\omega^2}{KT^2}(C_D + NTV + \frac{K_S B^2}{2V})\,\ddot{\theta} + \omega^2\dot{\theta} + \omega^2\frac{V}{T}\theta = 0 \quad [13B]$$

$$N = M_f + M_1 \quad [14B]$$

$$\omega^2 = \frac{KT^2}{I_w + NT^2} \quad [15B]$$

The solution of Equation [13B] is given by Gaskell (13), as

$$\theta = C_1 e^{\lambda t} + e^{\mu t}\,(C_2 \sin\omega t + C_3 \cos\omega t) \quad [16B]$$

Equation [16B] indicates a region of stability when $\mu < 0$ and a region of instability where $\mu > 0$. At the condition for threshold instability $\mu = 0$, and for a third-order differential equation of the general form,

$$\dddot{\theta} + A\ddot{\theta} + B\dot{\theta} + C\theta = 0 \quad [17B]$$

the exponents in Equation [16B] for threshold instability are

$$\mu = 0,\ \lambda = -C/B = -V_c/T \quad [18B]$$

and for Equation [17B]

$$AB = C \quad [19B]$$

Here the wheelchair velocity at the threshold of instability will be defined as the critical velocity V_c. Applying Equation [19B] to [13B] gives

$$C_D + \frac{K_S B^2}{2V_c} = \frac{V_c}{T} I_w \quad [20B]$$

Substituting [18B] and $\mu = 0$ into [16B], resluts in

$$\theta = C_1 e^{-\frac{V_c}{T}t} + C_2 \sin\omega t + C_3 \cos\omega t \quad [21B]$$

$$\dot{\theta} = -C_1\frac{V_c}{T}e^{-\frac{V_c}{T}t} + C_2\omega\cos\omega t - C_3\omega\sin\omega t \quad [22B]$$

$$\ddot{\theta} = C_1\frac{V_c^2}{T^2}e^{-\frac{V_c}{T}t} - C_2\omega^2\sin\omega t - C_3\omega^2\cos\omega t \quad [23B]$$

During the testing of wheelchair caster shimmy, the onset of caster shimmy was initiated by striking the caster with a mallet. An impact force of short duration will cause the caster wheel to deflect as well as impart an initial lateral velocity, thus at $t = 0$

$$\theta = \theta_o,\ \dot{\theta} = \dot{\theta}_o, \text{ and } \ddot{\theta}_o = 0 \quad [24B]$$

Using the boundary conditions of Equation [24B] in [21B], [22B], and [23B], the coefficients C_1, C_2, and C_3 can be determined as a function of initial conditions.

The solution to Equation [13B] is

$$\theta = \frac{\theta_o\frac{\omega^2T^2}{V_c^2}e^{-\frac{V_c}{T}t}}{1 + \frac{\omega^2T^2}{V_c^2}} + \left(\frac{\theta_o}{\omega} + \frac{\theta_o\frac{\omega T}{V_c}}{1 + \frac{\omega^2T^2}{V_c^2}}\right) \times \sin\omega t + \frac{\theta_o}{1 + \frac{\cos\omega^2T^2}{V_c^2}}\cos\omega t \quad [25B]$$

Equation [25B] can be simplified for caster wheels where $\omega T/V_c >> 1.0$, giving

$$\frac{\theta}{\theta_o} \cong e^{-\frac{V_c}{T}t} + \left(\frac{\dot{\theta}_o}{\omega\theta_o} + \frac{V_c}{\omega t}\right)\cos(\omega t - \phi) \qquad [26B]$$

Where

$$\tan\phi = \frac{\dfrac{\dot{\theta}_o}{\omega} + \dfrac{\theta_o \dfrac{\omega T}{V_c}}{1 + \dfrac{\omega^2 T^2}{V_c^2}}}{\dfrac{\theta_o}{1 + \dfrac{\omega^2 T^2}{V_c^2}}} \qquad [27B]$$

If $\dot{\theta}_o/\omega$ is negilgible, then the phase angle is given by

$$\tan\phi = \frac{\omega T}{V_c} \qquad [28B]$$

In Appendix C it will be shown that the term $\dot{\theta}_o/(\omega\theta_o)$ can be neglected in [26B], giving

$$\frac{\theta}{\theta_o} \cong e^{-\frac{V_c}{T}t} + \frac{v_c}{\omega T}\cos(\omega t - \phi) \qquad [29B]$$

Equation [29B] is the final form of the equation for predicting the shimmy motion of a wheelchair caster wheel.

APPENDIX C

CORRELATION OF CASTER SHIMMY THEORY WITH EXPERIMENT

A. Equivalent Damping Coefficient for Friction Damper

In Appendix B, the equations of motion for the caster wheel were derived assuming a hydraulic damper acting at the fork spindle. Wheelchairs use friction dampers at the fork spindle or simply rely on the friction of the spindle bearings for damping. It is possible to develop an equivalent damping coefficient for a friction damper following the method presented by Thomson (14). The method involves calculating the work-per-cycle of a frictional damper and setting this equal to the work-per-cycle for a hydraulic damper.

Assuming sinusoidal motion of the caster, the work-per-cycle of a frictional damper can be calculated as follows (where θ_a is the angular amplitude of the vibrating caster wheel about the spindle axis):

$$\text{Work} = 2M_f\theta_a\int_o^{\pi} \sin\omega t\, d(\omega t) \qquad [1C]$$

$$= 4M_f\theta_a$$

For the hydraulic damper, the work-per-cylce can be calculated as follows:

$$\text{Work} = C_D\omega^2\theta_a^2\int_o^{2\pi/\omega} \cos^2(\omega t)\, dt \qquad [2C]$$

$$= \pi C_D\omega\theta_a^2$$

Setting the work in Equation [1C] equal to [2C] get

$$C_D = \frac{4M_f}{\pi\omega\theta_a} \qquad [3C]$$

B. Critical Velocity for Shimmy

In Appendix B the equations for the self-excited motion of the caster wheel at the threshold of instability were derived, resulting in Equation [20B], where

$$C_D + \frac{K_s B^2}{2V_c} = \frac{V_c}{T} I_w$$

Substituting for C_D from the equation for frictional damping [3C] get

$$\frac{4M_f}{\pi\omega\theta_a} + \frac{K_s B^2}{2V_c} = \frac{V_c}{T} I_w \qquad [4C]$$

From [26B] the steady-state amplitude of vibration is

substituted into Equation [4C], giving

$$\frac{4M_f}{\pi\theta_o\left(\frac{\dot{\theta}_o}{\theta_o}+\frac{V_c}{T}\right)}+\frac{K_sB^2}{2V_c}=\frac{V_c}{T}I_w \qquad [5C]$$

Bruning (7) measured the vibration of the caster wheel at different wheelchair speeds, and the results for a particular test are shown in Figure 1C. In this example the steady-state amplitude of vibration was found to be $\theta_a = 8$ degrees $= 0.14$ radians. Carefully examining the trace at the instant the caster wheel was struck with a rubber hammer shows that there is an initial displacement on the order of $\theta_o = 20$ degrees $= 0.35$ radians. From Equation [26B] the steady-state amplitude is

$$\theta_{a(s.s.)}=\frac{\dot{\theta}_o}{\omega}+\frac{\theta_o}{\frac{\omega T}{V_c}} \qquad [6C]$$

For $V_c = 2.53$ m/s, $\omega = 104.7$ radians/sec, and trail

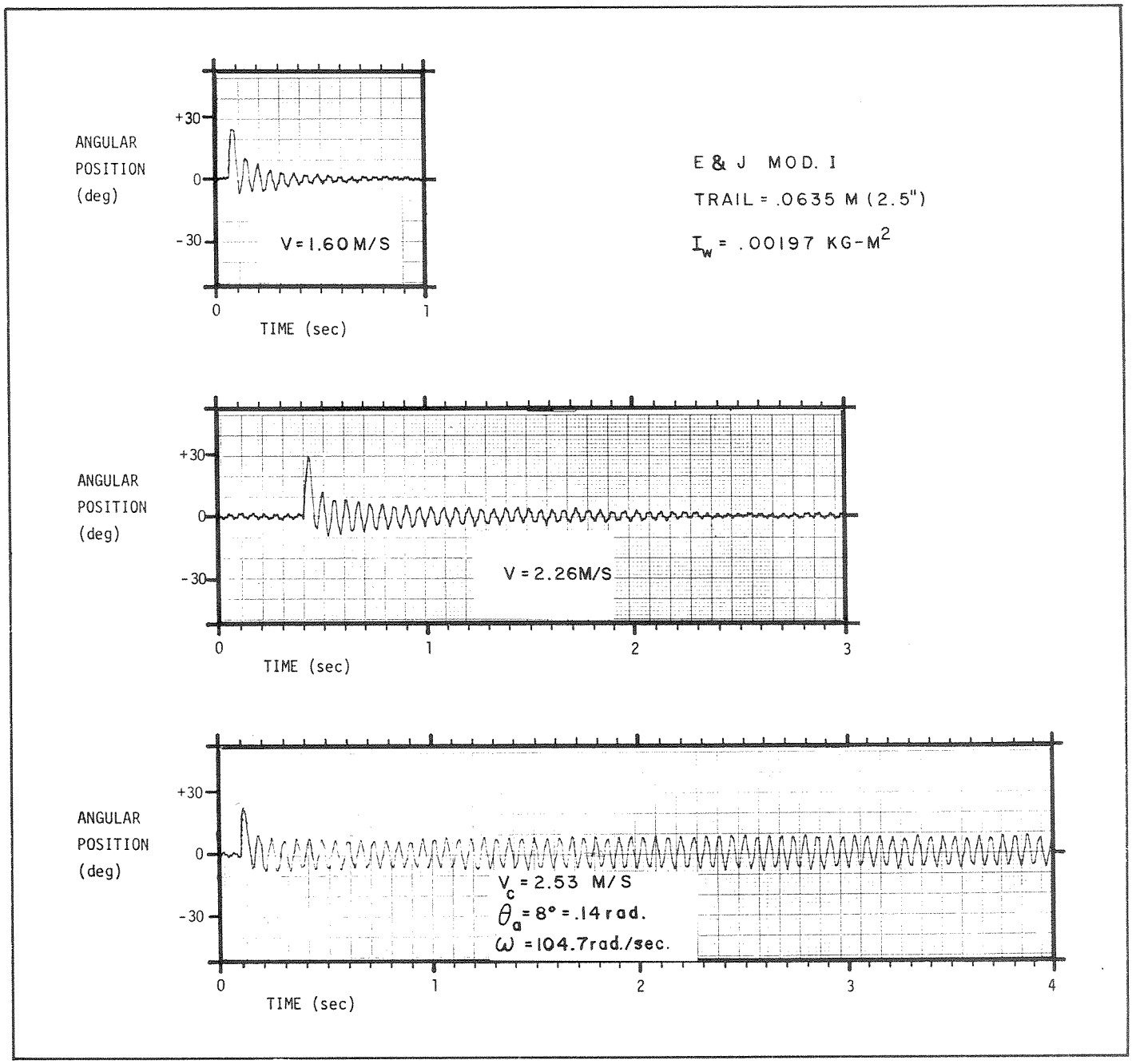

FIGURE 1C
Caster wheel oscillation versus wheelchair speed.

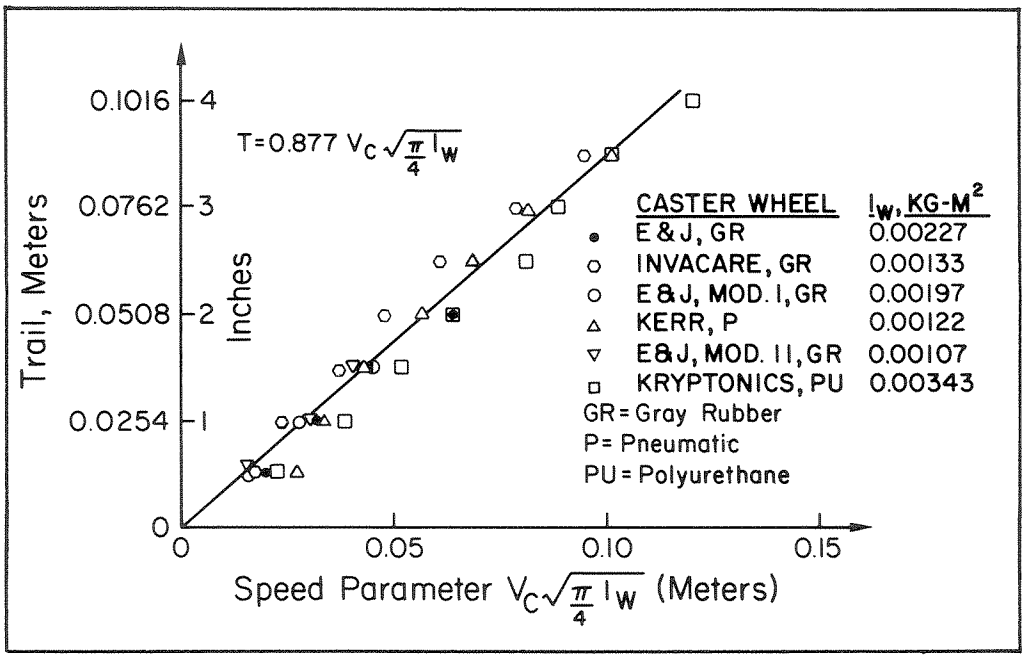

FIGURE 2C
Correlation of caster shimmy data with theory.

equals 2.5 inches = .0635 meters, Equation [6C] gives

$$\dot{\theta}_o = \theta_a\omega - \theta_a\frac{V_C}{T} = .14\,(104.7) - \frac{.35\,(2.53)}{.0635} \quad [7C]$$

$$= .7 \text{ rad/sec}$$

In the damping term of Equation [5C] we have

$$\frac{\dot{\theta}_o}{\theta_o} + \frac{V_C}{T} = \frac{.7}{.35} + \frac{2.53}{.0635} = 2.0 + 39.8 \quad [8C]$$

Since the term $\theta_o/\theta_o >> V_C/T$ as shown in Equation [8C], this term will be neglected. Thus Equation [5C] becomes

$$\frac{4M_fT}{\pi\theta_o V_C} + \frac{K_sB^2}{2V_C} = \frac{V_C}{T} I_W \quad [9C]$$

Solving for V_C get

$$V_C = \sqrt{\frac{4M_fT^2}{\pi\theta_o I_W} + \frac{K_sB^2T}{2\,I_W}} \quad [10C]$$

In order to fit the theory [10C] with experiment, several caster shimmy tests reported by Bruning (7) were plotted and an overall M_f/θ_o calculated. The plot of this data is shown in Figure 2C and includes gray rubber and polyurethane solid tires as well as a pneumatic tire. Fitting a curve to the data gives

$$\frac{M_f}{\theta_o} = 1.3 \quad [11C]$$

The slip coefficient K_s must be evaluated in order to apply Equation [10C] to a grooved tire or co-rotating caster wheels.

From Equation [1B] we have

$$F_T = K_s\frac{\Delta V}{V} \quad [12C]$$

A polyurethane tire caster wheel with a load of 178N (40lb) was held at several fixed angles with respect to the travel of a treadmill belt and F_T, ΔV, and V measured. The results are shown in Figure 3C for V = 2 km/hr. The slope of the curve gives K_s, where it was found that K_s = 1250 newtons. Results for other speeds, tire materials, and loads did not change K_s significantly.

Using Equation [12C] gives good results when applying Equation [10C] to grooved-tread caster wheels as shown by the dashed lines in Figures 3 and 4 on page 17.

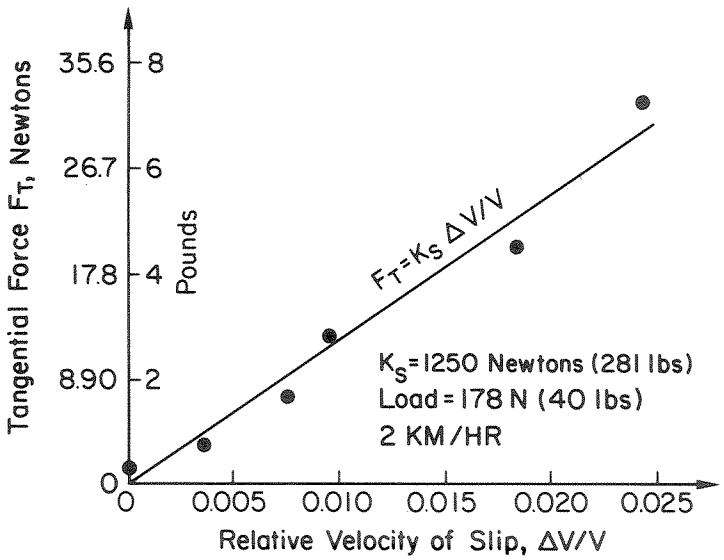

FIGURE 3C
Caster wheel slip coefficient.

APPENDIX D

Nomenclature

a	distance to C.G., m
A	coefficient
b	distance to C.G., m
B	coefficient and tread separation, m
$C_{1,2,3}$	coefficients
C	coefficients
C_D	damping coefficient, N-m/rad/sec
d	diameter, m
F	force, N
F_c	Caster force to turn, N
F_x	horizontal force, N
F_y	vertical force, N
F_T	tangential force, N
F_N	normal force, N
h	threshold height, m
I_w	mass moment of inertia of wheel about a diameter, kg-m^2
I_g	mass moment of inertia of caster, kg-m^2
K	spring constant, N/m
K_s	slip coefficient, N
L	load, N
M_1	mass of bearing housing, kg
M_C	mass of caster, kg
M_F	mass of fork, kg
M_{F_T}	moment, N-m
M_f	friction moment, N-m
M_w	mass of wheel, kg
M_{Twist}	wheelchair turning moment, N-m
N	floor reaction, N
P	force, N
R	threshold reaction, N
t	time, sec
T	trail, m
V	wheelchair velocity, m/sec
V_c	critical velocity, m/sec
ΔV	change in velocity, m/sec
W	width between rear wheels,m
X	displacement or distance between wheels, m
$\dot{X}$	velocity, m/sec
$\ddot{X}_G$	acceleration of C.G., m/sec^2
$\dddot{X}$	acceleration, m/sec^2
Δ	distance from force to wheel pivot point, m
θ	angular displacement, rad
θ_o	initial angular displacement, rad.
$\dot{\theta}$	angular velocity, rad/sec
$\ddot{\theta}$	angular acceleration, rad/sec^2
$\dddot{\theta}$	angular jerk, rad/sec^3
θ_a	angular amplitude, rad
λ	exponent in Eq. (2), sec^{-1}
μ	exponent in Eq. (2), sec^{-1}
ϕ	phase lag, rad.
ω	frequency, rad./sec.

REFERENCES

1. Kauzlarich JJ, Bruning TE, and Dimaio WG: A New Solution to Caster Wheel Shimmy. **In** Proceedings of the 6th Annual Conference on Rehabilitation Engineering, San Diego, California, June 12-16 1983, pp. 109-111.
2. Bruning TE, Kauzlarich JJ, and McLaurin CA: The Effect of Inertial Parameters of Casters on Wheelchair Caster Shimmy. **In** Proceedings of 6th Annual Conference on Rehabilitation Engineering, San Diego, California, June 12-16 1983, pp. 112-114.
3. Brearley MN: Investigation of Caster Wheel Shimmy. Quart J Mech & Appl Math 33(4):491-505, 1980.
4. Brearley MN: Caster wheel shimmy and its prevention. Technical Aid to the Disabled Journal 3(4):43, 45, Dec 1983.
5. Kauzlarich JJ: Analysis of Wheelchair Caster Shimmy. **In** Proceedings of the 7th International Conference on Rehabilitation Engineering, June 17-22, 1984, Ottowa, Canada.
6. Thacker J: Increased Turning Torque Due to a Grooved Caster Wheel. **In** Proceedings of the 7th International Conference on Rehabilitation Engineering, June 17-22, 1984, Ottowa, Canada.
7. Bruning TE: Investigation of Wheelchair Caster Shimmy. Master's Thesis, University of Virginia, Mechanical Engineering Department, May 1982.
8. Smiley RF: Correlation, Evaluation, and Extension of Linearized Theories for Tire Motion and Wheel Shimmy. Technical Report 1299, NACA, 1957.
9. Stout G: Some Aspects of High Performance Indoor/Outdoor Wheelchairs. Bull Prosth Res, BPR 10-32, Fall 1979, pp. 135-175.
10. Kauzlarich JJ: Powered Wheelchair Performance Testing. **In** Wheelchair Mobility: A Summary of Activities at the University of Virginia REC, 1976-1981. UVa Rehabilitation Engineering Center, Charlottesville, Virginia 22903.
11. Moreland WJ: Landing Gear Vibration. **In** AF Tech Report 6590, Wright Air Develop, Center, Oct. 1951, pp. 70.
12. Stevens JE: Shimmy of a Nose-Gear with Dual Co-Rotating Wheels. J. Aerospace Sci 28:622-630, Aug 1961.
13. Gaskell RE: Engineering Mathematics. New York, Dryden Press, 1958.
14. Thomson WT: Theory of Vibration with Applications, 2nd. Edition, Englewood Cliffs, New Jersey, Prentice-Hall, 1981